Chapter 12

Vacuum system

V. Baglin[1*], *P.* Chiggiato[1], *C. Garion*[1] *and G. Riddone*[1]

[1]CERN, Accelerator & Technology Sector, Switzerland
[*]Corresponding author

12 Vacuum system

12.1 Overview

The luminosity upgrade programme (HL-LHC) requires modifications of the present LHC's vacuum system, in particular in the triplets, crab cavities, matching section and experimental areas. Such modifications must follow guidelines similar to those followed for the present machine. The increased stored current implies a higher thermal power in the beam screen from the image current moving along with the stored particles and stronger synchrotron radiation (SR) and electron cloud (EC) effects, which in turn translate into higher degassing rates.

One of the main tasks of the HL-LHC vacuum work package is to produce new beam screens in the new superconducting (SC) Inner Triplet (IT) and D1-D2 magnets together with the vacuum layout along the Insertion Region (IR). It is also necessary to assemble and insert with the beam screens high-density shielding material into IT magnets. This is mandatory for protecting the magnets from collision debris coming from the experiments' interaction points (IPs). A balance between cold bore size and vacuum pumping system is defined based on experience gained with the present machine and recent advances with new materials. Indeed, a number of new ideas have emerged recently for the mitigation of the e-cloud effect in cryogenic beam pipes: amorphous carbon (a-C) coating for which validation is ongoing and laser structured surface currently under study.

The change of the aperture of the IT at IR1 and IR5 implies that the experimental vacuum chambers of CMS and ATLAS require a review of aperture, impedance, and vacuum (dynamic and static). The forward regions of CMS and ATLAS will need to be adapted to cope with the new beam geometry in IR1 and IR5. New vacuum systems at the tunnel/cavern interfaces are needed to mitigate the additional activation from the increased luminosity. New access procedures and tooling will be also needed to allow the minimization of the integrated dose to personnel. With the HL-LHC, less flexibility will be available for the optics of LHCb and ALICE; therefore, the vacuum chambers at IR2 and IR8 must be validated for operating conditions to ensure that these chambers do not impose a limitation. *In-situ* a-C coating of the beam screens of the IT magnets, located in LSS2 and 8, is under validation to reduce the electron cloud heat load onto the cryogenic system. Finally, positions of mechanical supports, pumps, and gauges must be analyzed to ensure that layouts are optimized for the new machine configuration. Bake-out equipment will be redefined depending on activation and specific needs. To deliver good vacuum conditions, all chambers held at room temperature must be treated with Non-Evaporative Getter (NEG), to provide low dynamic outgassing with large pumping speed and to minimize secondary electron yield (SEY), to reduce electron cloud effects.

12.2 Beam vacuum requirements

The HL-LHC beam vacuum system must be designed to ensure the required performance when beams with HL-LHC nominal parameters circulate ($L_{peak} = 5 \times 10^{34}$ cm^{-2} s^{-1}, $L_{int} \sim 3$ ab^{-1}). By using engineering margins, the system must be designed for the HL-LHC ultimate performance ($L_{peak\ ult} = 7.5 \times 10^{34}$ cm^{-2}s^{-1}, $L_{int\ ult} \sim 4$ ab^{-1})[1].

The vacuum system must be designed

- to avoid pressure runaway induced by ion-stimulated desorption,
- to satisfy the vacuum lifetime,
- and to provide low background to the experiments induced by beam-gas collisions.

The design considers the effects of synchrotron radiation, electron cloud, and ion-stimulated desorption from the walls. Heat load onto the beam vacuum chamber walls or flanges and beam impedance effects must also be taken into account [2].

The system must be compatible with the global LHC impedance budget and the designated machine aperture.

The average gas density along the ring must satisfy a maximum level of heat load into the cold mass as defined by the 100 h vacuum lifetime due to nuclear scattering, i.e. less than 1.2×10^{15} H_2 molecules m^{-3} equivalent in the LHC [3]. The corresponding heat load into the cold mass is therefore limited to ~ 80 mW/m when both beams circulate. Since this acceptable gas density limit decreases proportionally to the inverse of the beam current, the HL-LHC vacuum lifetime is set to 200 h. Table 12-1 gives the molecular gas densities yielding a 100 h vacuum lifetime in the LHC and 200 h vacuum lifetime in the HL-LHC assuming the presence of a single gas species in the vacuum system.

Table 12-1: Single gas species molecular gas density (m−3) to satisfy 100 h vacuum lifetime in the LHC and 200 h vacuum lifetime in the HL-LHC [3].

Machine	**I** **A**	**H_2** **m^{-3}**	**CH_4** **m^{-3}**	**H_2O** **m^{-3}**	**CO** **m^{-3}**	**CO_2** **m^{-3}**
LHC	0.58	1.2×10^{15}	1.8×10^{14}	1.8×10^{14}	1.2×10^{14}	7.9×10^{13}
HL-LHC	1.09	6.4×10^{14}	9.6×10^{13}	9.6×10^{13}	6.4×10^{13}	4.2×10^{13}

The average gas density along IR1, IR2, IR5, and IR8 must also ensure that the background to the LHC experiments remains at acceptable levels [4][5]. In the absence of specified values from the LHC experiments themselves, the LHC design value will be scaled to the HL-LHC parameters as shown in Table 12-2 where the gas density is expressed in H_2 equivalent. Therefore, for HL-LHC, the designed average gas density in the IR1&5 (mainly dominated by the cryo-elements and other beam equipment such as collimators, masks etc.) equals 2.8×10^{12} H_2 equiv/m^3 which correspond to a pressure of 1×10^{-10} mbar assuming the solely presence of hydrogen in the vacuum system.

Table 12-2**:** H_2 equivalent gas density (H_2 equiv/m^3) design value for the LHC high luminosity experiment and IRs [4][5]and for the HL-LHC.

Machine	**I** **A**	**ATLAS** **H_2 equiv/m^3**	**CMS** **H_2 equiv/m^3**	**IR1&5** **H_2 equiv/m^3**	**IR2&8** **H_2 equiv/m^3**
LHC	0.58	1.5×10^{11}	3.1×10^{12}	5.3×10^{12}	6.5×10^{12}
HL-LHC	1.09	8.0×10^{10}	1.6×10^{12}	2.8×10^{12}	3.5×10^{12}

12.3 Vacuum layout

The vacuum layout must ensure the vacuum requirements for circulating beams with the HL-LHC nominal parameters. The system must be designed for the HL-LHC ultimate luminosity, without margin.

- All beam vacuum elements must be leak tight (leak rate less than 10^{-11} mbar. ℓ/s He equivalent), clean according to CERN vacuum standards, and free of contamination *e.g.* grease, oil, fingerprints.
- According to the LHC baseline [3], the vacuum system in the Long Straight Sections (LSS) must be sectorized with gated valves, see in Figure 12-1 a schematic of the HL-LHC sectorisation on the left side of IP1 and 5. The vacuum sectorization is delimited by cold-to-warm transitions, length of vacuum sectors, or specificity of components (fragility, maintenance, etc.) [6].
- Vacuum sector valves must be installed at each cold-to-warm transition in order to decouple the room temperature and cryogenic temperature vacuum systems during bake-out, cool-down, installation, and commissioning phases.
- The distance between the vacuum sector valve and the cold-to-warm transition must be minimized in order to reduce the length of the beamline that is not baked-out in situ.
- Dedicated vacuum instrumentation must be provided close to and on both side of each sector valve for beam interlocking and along any vacuum sector for diagnostics.
- Sector valves must be remotely controlled and interlocked in order to dump the circulating beam in the case of malfunctioning. The LHC and the HL-LHC vacuum sectorizations delimit two types of vacuum system:
    - room temperature vacuum system,
    - cryogenic temperature vacuum system.

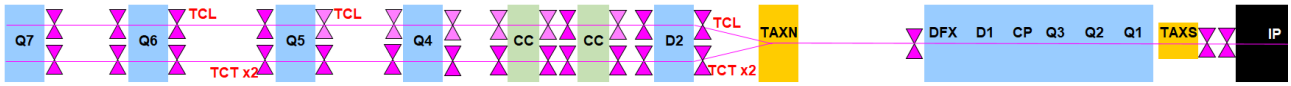

Figure 12-1: Schematic of the HL-LHC vacuum sectorisation of all the cryo-elements from the interaction point (IP) to Q7.

- The vacuum system shall be integrated in the tunnel and cavern volumes with the permanent/mobile bake-out system, bake-out racks, quick flanges collars, mobile pumping systems, and diagnostics systems. The corresponding space must be reserved into the tunnel integration to allow a proper access and operation of the vacuum system. At present, detailed studies were conducted for the TAXS, DFX, TAXN-D2 and CC areas, see e.g.[48].
- Integration studies must also be performed for installation and un-installation phases of equipment to identify potential conflicts.
- Integration and installation drawings must be circulated and validated before installation in the tunnel and caverns.
- The vacuum chamber aperture is defined by the beam optics system, the beam impedance, by machine protection, and background considerations of the experiments. The aperture of the vacuum chamber must not be the limiting aperture [49].
- All components to be installed into the vacuum systems must be approved and their vacuum performance validated before installation.
- A maximum number of LHC beam vacuum components will be reused for the HL-LHC upgrade. The present vacuum layout design foresees to reuse about 56 sector valves, 120 vacuum chambers and 144 vacuum modules.

- High radiation areas along the LSS identified at an early stage of the design, highlighted positions where remote handling/tooling might be preferred and positions where instrumentation must be radiation resistant [15]. The present vacuum layout design foresees remote handling in the TAXS area (see Section 12.5) and remote tooling for the DFX and TAXN-D2 areas.
- When needed, irradiation tests of specific components (instruments, bake-out jackets, cables, electronics, O-rings, etc.) must be conducted to demonstrated that they meet the radiation dose specifications.
- The vacuum work package spares policy follows the general A&T sector policy. The defined spares policy benefits from large quantity orders, in particular for highly specialized equipment such as beam screens, cold bores, cold warm transitions and standard equipment such as modules, vacuum chambers, sector valves etc [20].
- Similar to the LHC construction, cryogenic elements must be installed first, then room temperature vacuum sector valves, followed by completion of the room temperature vacuum sectors.
- Time, resources, and space to allow the temporary storage of LHC vacuum components, which need to be dismounted to allow the HL-LHC infrastructure modifications and equipment installation, will be evaluated in the next phase of the project.

12.3.1 Room temperature vacuum system

Standard vacuum chambers and vacuum modules will connect the machine components. Similar to the LHC vacuum system, all components must be bakeable (230°C ±20°C for NEG coated vacuum chambers and 300°C ±20°C for uncoated stainless-steel beam pipes). The vacuum system layout is designed to fulfil the stated requirements throughout a full run [3][25].

The current LHC circular vacuum chambers variants are 80 mm, 100 mm, 130 mm, and 212 mm ID: any further variants needed for the HL-LHC will be kept to the minimum necessary. The present HL-LHC vacuum layout, still under development, requires the introduction of 150 mm, 250 mm ID as new circular vacuum chamber standard to accommodate the required beam aperture between D1 and D2 [21].

An exception is the recombination chambers installed into the TAXN absorber, which by definition is not circular. The present HL-LHC recombination chamber, still under development, is based on two 88 mm ID chambers, installed coaxially to the beam path, merging into a 250 mm ID chamber [22].

Vacuum chamber transitions (VCT), which give offsets and adaptations between pipe apertures, must be integrated into the concerned equipment by the equipment owners themselves at the early design stage, e.g. beam monitors, superconducting cavities, quadrupole masks, etc. in agreement with the vacuum, surface and coating group of the CERN Technology department. The present HL-LHC vacuum layout requires the production of 4 VCTs to accommodate 250/212 mm apertures and 212/150 mm apertures.

The vacuum chambers are aligned within ±3 mm accuracy. Better tolerance will require the installation of survey targets on the vacuum chamber, their fiducialisation and their alignment with the support of the survey team. In this latter case, the vacuum equipment may be aligned within ±0.2 mm accuracy at best. Alignment of other equipment is the responsibility of the survey team.

Remotely aligned components require a radial stroke of ±2.5 mm by design. Therefore, all transitions between remotely aligned components and fixed components shall have a deformable RF bridge. The present vacuum layout design foresees two remotely aligned sector valve assemblies located upstream and downstream to D2. The other vacuum components have large enough apertures to remain fixed to the ground or are supported by remotely aligned components to be compatible with the full remote alignment system (FRAS) [50][51].

The supporting system of the new HL-LHC room temperature vacuum component is based on an upgrade version of the LHC supporting system, ALARA approach and FRAS requirements. Specific supports

are under design for new vacuum chamber standards, vacuum components located next to deformable RF bridges and remotely aligned sector valve assemblies. Upgraded supports are foreseen for some LHC-like sector valve assemblies and vacuum chambers. In the ALARA context, some supporting system may be aligned during initial installation and allow a disconnection / reconnection of the vacuum device without further re-alignment.

The choice of the vacuum chamber material between Cu-alloy and stainless steel (either Cu coated or bare) is dictated by beam impedance and production constraints. In the LHC, ID apertures up-to 130 mm are made of bulk Cu. Al- alloys are preferred in high-radiation areas.

Connections between equipment must be made by ConFlat® bolt technology unless radiation issues and/or remote handling require the use of quick-release flanges with, for example, chain clamps.

12.3.2 Cryogenic temperature beam vacuum system

The cryogenic beam vacuum system must be tightly decoupled by sector valves from the room temperature vacuum system. Dedicated instruments must be provided close to the sector valves to allow atmospheric evacuation roughing, monitoring, and safety against overpressure of the beam vacuum vessel.

A cold-to-warm transition must be integrated into the cryogenic beam vacuum sector at each extremity of the cryogenic system.

A continuous cold bore, i.e. without penetrating welds between the beam vacuum and helium enclosure, ensures leak-tightness between the superfluid helium and beam vacuum along the cryogenic beam vacuum sector. The LHC nominal cold bore temperature is 1.9 K in the arcs.

A beam screen must be inserted into the cold bore to extract the beam-induced heat load at a temperature higher than 1.9 K. The beam screen must be perforated with slots (4% transparency in the LHC arcs) to allow pumping into the cold bore space [3]. The LHC beam screen operates from 5 K to 20 K. The HL-LHC beam screens of the IT quads, corrector package and D1 will operate at a higher temperature, between 60 K and 80 K [52], to cope with the much higher heat load (15–25 W/m). When required, in situ heating of the LHC beam screen up to 90 K, with cold bore < 3 K, is used to flush the condensed gas present on the beam screen inner surfaces towards the cold bore. Owing to the presence of a-C coating, the value is increased to 120 K for the HL-LHC beam screens [52]. This heating cycle may be performed after a long technical stop or even between physics fills. For the new beam screens built for the HL-LHC project, the surface area of the beam screen perforation will be scaled to the HL-LHC parameters, hence doubled, and therefore increased as compared to the LHC.

When a cold bore operates at 4.5 K, cryo-absorbers are installed outside the beam screen in order to provide hydrogen pumping speed and capacity [3]. Cryo-absorbers are mandatory for cold bores operating above 2.8 K. Cryo-absorbers shall be placed outside the beam screen and thermally anchored on it. In situ heating of the beam screen up to 90 K is required for the cryo-absorbers regeneration [3].

In the cold part of the LHC, the maximum length without beam screen is less than 1 m (with the exception of superconducting cavities). This LHC design value will be scaled to the HL-LHC parameters and therefore reduced.

For the HL-LHC, the beam screen aperture is derived from beam optics and magnet aperture inputs, for details see Table 12-3 and Table 12-4 in the beam screen design section.

12.4 Insulation vacuum

The insulation vacuum system ensures the performance of the cryogenic system by eliminating the heat losses due to gas convection. The insulation vacuum systems under the responsibility of TE-VSC include the cryogenic distribution line (QRL) and cryogenic machine components up to a vacuum barrier, but exclude transfer lines outside the LHC tunnel and those of the experimental cavern, unless specifically agreed with the equipment owner.

The requirements of the insulation vacuum system for the HL-LHC can be summarized as follows:

- the pressure must be below 10^{-5} mbar;
- the helium leak rate, at the component level, must be below 10^{-10} mbar ℓ/s;
- it must be compatible with the LHC insulation vacuum system [3];
- it must be built with the same standards used for the LHC insulation vacuum system.

The QRL and the magnet cryostats are mechanically connected via specific bellows and pipes assemblies called jumpers. However, the insulation vacuum of the QRL and continuous cryostat is sectorized through vacuum barriers. There is no sectorization of the QRL in the LSS of the LHC. Sectorization of the HL-LHC cryostats shall ensure that longitudinal leak location techniques can be employed. Connection to cryo-plant or transfer lines outside the LHC tunnel shall be delimited by vacuum barriers.

Figure 12-2 shows, for the present baseline, a schematic of the insulation vacuum equipment which is under the scope of WP12. These components are in connection with the beam vacuum on one side and delimitated by a vacuum barrier on the other side. Equipment over the vacuum barrier are outside the scope of WP12. The purpose of this geographical separation is to ensure that any malfunctioning of an insulation vacuum sector, under the responsibility of VSC, will not alter the beam vacuum performance. The present layout, still under study, foresees the creation of 11 insulation vacuum subsectors per IP side (the LHC has only 5 insulation vacuum sectors per IP side).

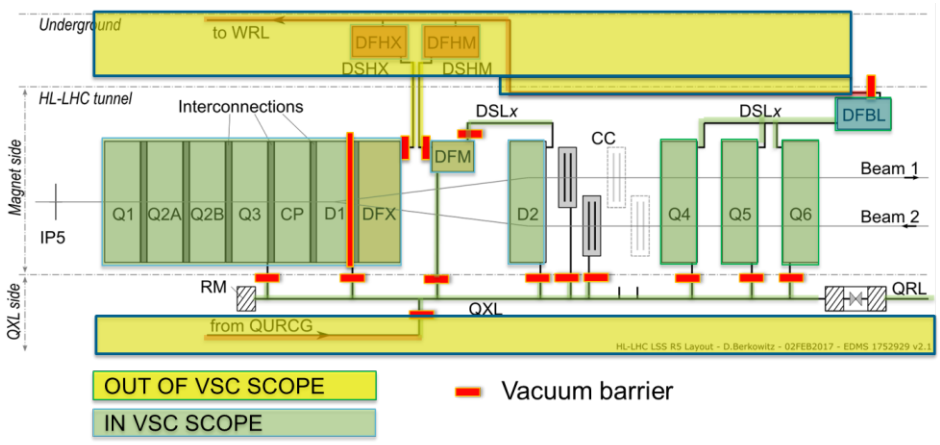

Figure 12-2: Schematic of the HL-LHC insulation vacuum layout. Insulation vacuum equipment under the VSC scope (defined by the vacuum barrier position) are highlighted in green.

The insulation vacuum relies on cryopumping during normal operation. Fixed turbomolecular pumping groups are used for pumping before cool-down. This system also mitigates the impact of possible helium leaks during operation, therefore runs constantly. Such pumps are also used for the detection of helium or air leaks. Dedicated pumping ports are employed for rough pumping groups, pressure gauges, pressure relief valves, longitudinal leak localization techniques, and additional pump placement in case of operational leaks. A bypass equipped with isolation valves is installed between subsectors. The standard for pumping ports is the ISO-K DN 100 flange. Each insulation vacuum volume must be equipped with pressure relief valves. Elastomer seals (Viton, NBR) are used where system disassembling is necessary (interconnections, instrumentations, etc.).

For the HL-LHC project, in high radiation areas, specific seals (metals or hard-rad polymers) have to be installed on new equipment and be used to replace standard seals on any retained equipment.

12.5 Experimental vacuum system

The experimental vacuum system is located between Q1L and Q1R of each interaction point. Similarly to the LSS, the vacuum layout of each experimental vacuum system must ensure the vacuum requirements when

beams with the HL-LHC nominal parameters circulate. The system shall be designed for the HL-LHC ultimate performance, without margin [25]. Therefore, all constraints and requirements defined in Section 12.3 apply also in this Section.

During long beam stops (> 10 days), ultra-pure neon venting is needed to protect the fragile experimental vacuum chambers from deformations caused by possible mechanical shocks. The baseline is that there will be no work in the vicinity of the vacuum chambers while they are under vacuum.

The vacuum chamber supporting system must be compatible with standard activities performed in the experimental cavern during short stops (e.g. winter technical stops). In particular, no personnel are allowed in the vicinity of the beam pipe (< 2 m radius) during these phases.

As for the present LSS vacuum system, all machine components operating at room temperature must be bakeable and NEG coated.

Accidental or scheduled air venting for repair or maintenance of any of the vacuum sectors of the experimental vacuum system implies a complete NEG recommissioning of the beam pipes, i.e. two bake-out cycles, the first for the bake-out of the metallic part, the second for NEG activation.

12.5.1 High luminosity experiments: ATLAS and CMS

ATLAS and CMS LHC vacuum layout drawings are described in Refs. [7] and [8] and not discussed here. The secondary particles absorber, TAXS, is located at the interface between the tunnel and the experimental cavern.

At the tunnel extremity, as shown in Figure 12-3, left side, the instrumentation of the Q1–TAXS areas is minimized to prevent from personnel access after the installation. The present baseline foresees a simple connecting bellow and two ion pumps between Q1 and TAXS chambers. The connecting bellow is surrounded by an insulating vacuum to minimise the impact of potential leaks into the beam vacuum system.

At the cavern extremity, a complete and robust decoupling between the two complex and delicate IT and experimental vacuum sectors, is obtained by two vacuum sector valves sitting almost side by side, see Figure 12-3, right. The vacuum sector defined by these two sector valves is named hereafter ‘buffer’.

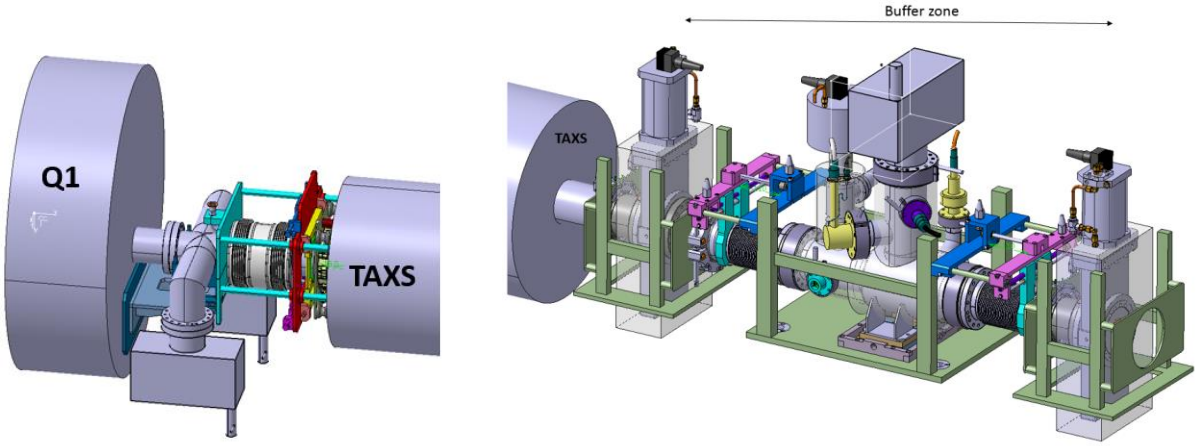

Figure 12-3: Schematic of the HL-LHC high luminosity experiments instrumentation areas. Left, connection between Q1 and TAXS. Right, buffer zone between sector valves.

On both sides of ATLAS and CMS caverns, a vacuum system is installed in the buffer zone to allow neon venting, pump-down and vacuum commissioning during NEG activation of the ATLAS and CMS experiment. A rupture disk is also installed in this system to protect the experimental vacuum chambers in case of liquid helium inrush.

The following are required to avoid personnel intervention in a high radiation area:

- A pumping and neon venting systems will be installed in the buffer zone on both sides of ATLAS during LS3 to complement the left-hand side [9].
- Remote tooling and handling are foreseen to avoid personnel intervention [15]. Quick type flanges are mandatory. Welds are preferred to flanges.
- Installed components must be robust: in particular, sliding fingers in RF bridges are forbidden.

The bake-out system must be permanent and fully integrated with the other systems from the design phase.

It is assumed that the ATLAS central beam pipe inner diameter, as installed during LS1, remains the same until at least LS4 [9].

According to Ref. [10], the following are assumed.

- The CMS central beam pipe inner diameter, as installed during LS2 remains the same until at least LS4.
- End cap, HF, CT2, and forward pipes of the CMS vacuum system will be upgraded to Al bulk material during LS2. No mechanical intervention between +/- 16 from the IP is therefore expected during LS3.
- A permanent bake out system will be installed at CMS during LS2, with the exception of the central Be chamber.

Since the TAS needs to be replaced during LS3, and a new 'buffer zone' will be installed, the vacuum system located inside the experimental cavern needs to be adapted and recommissioned, i.e. requiring NEG activation even if no changes to the vacuum system inside the cavern is foreseen.

12.5.2 ALICE and LHCb experiments

ALICE and LHCb vacuum systems are not part of the HL-LHC upgrade. However, their vacuum system is still upgraded during LS2 and LS3. The interested reader may refer to Refs. [11][12][13] and [14] for detailed documentation.

12.6 Beam screen design

Beam screens are inserted into cryogenic cold bores to guarantee the vacuum performance. They are part of the LHC vacuum system baseline [1]. The HL-LHC beam screen must be compatible with vacuum, impedance and cryogenic, including e-cloud, requirements of LHC [3][25].

In order to operate properly, the beam vacuum system must be evacuated, before cool-down, for, at least, five consecutive weeks, to allow the outgassing rate of adsorbed water to be reduced to acceptable levels.

During cool-down of a cryogenic system, the cold bore must be cooled first to minimize gas condensation onto the beam screen.

In the case where gas condenses onto the beam screen during operation, e.g. after a magnet quench, a transfer of this gas towards the cold bore via beam screen heating may be needed. This procedure should be carried out in a couple of days.

The HL-LHC beam screen must be inserted during the cryostating phase prior to tunnel installation. The surface of the beam screens must be kept clean during assembly. This implies that the beam screen is installed at the last stage of cryostating. Without specific tooling, procedures and approval from the vacuum group, no probe or device can be inserted into the vacuum system once the beam screens are installed.

The cooling tubes must be dimensioned to allow a proper cooling of the system during operation within the limits defined above.

According to vacuum standards, full penetrating welds are forbidden in the vessel wall separating the beam vacuum and helium enclosures.

Depending on the location, two types of beam screens exist: shielded and non-shielded beam screens. The shielded beam screens intercept part of the debris produced at the high luminosity IPs, thereby protecting the cold masses from radiation-induced damaged. In Q1, the beam screen surface shall withstand a dose of 1 GGy during its lifetime.

The selected beam screen material is P506 non-magnetic stainless steel, same material as present LHC beam screens. Copper is co-laminated with the stainless steel for impedance reasons. The thickness of the Cu layer is 75 μm.

Amorphous carbon (a-C) coating is the baseline for the inner surface of the HL-LHC shielded and non-shielded beam screens. Due to a-C's properties, electron multipacting suppression in these HL-LHC components and photon stimulated gas load comparable to copper are expected [26][27]. Amorphous carbon coating will be applied to the HL-LHC beam screens when needed for the reduction of heat load to cryogenic systems, reduction of background to experiment, and/or beam physics requirements.

The present state of the art of the in-situ coating process has led to the decision to produce during LS2 a-C coating of beam screens located in Q5R2, Q6R2, Q6L8 and Q5L8 of the LHC [23]. The parameters used for this coating are a first layer of 150 nm thick Ti, to provide adherence and to reduce the beam screen outgassing during coating, and a 50 nm thick, top layer of carbon. During the deposition of the carbon layer, Ti is also deposited to provide pumping during the coating process of hydrogen and water molecules to keep the maximum secondary electron yield below 1.1. The overall thickness of the Ti layer will not exceed 500 nm in order to maintain the overall impact on impedance negligible [24].

Amorphous carbon coating shall be the last step of beam vacuum preparation before lowering the magnet into the tunnel, avoiding any subsequent insertion of tooling or other devices into the beam vacuum line.

For IP2 and IP8, in situ coating of the present beam screen (or alternatively laser surface structuring) must be studied and conducted during the long shutdown (LS2 and LS3). If in situ coating or other treatments are not possible, removal of the magnet cryostat will be considered to allow beam screen exchange. The present baseline foresees the in-situ coating of the four ITs and six standalone magnets, namely D1Q3Q2Q1L2, D1Q3Q2Q1R2, D2Q4R2, Q5R2,Q6R2, Q6L8, Q5L8, D2Q4L8, D1Q3Q2Q1L8, D1Q3Q2Q1R8 [28].

For IP1 and IP5, new beam screens will be coated during RUN 3 and reused beam screen will be coated at the surface during LS3 for upgrade of the magnets. The present baseline foresees the coating of the following new magnets: D2L1, D1CPQ3Q2Q1L1, D1CPQ3Q2Q1R1, D2R2 and D2L5, D1CPQ3Q2Q1L5, D1CPQ3Q2Q1R5, D2R5. The coating of the LHC upgraded magnets is planned for Q5L1, Q4L1, Q4R1, Q5R1 and Q5L5, Q4L5, Q4R5, Q5R5 [28]. The beam screens of the non-crabbed beam pipes inside the crab-cavity cryomodules are also coated [53].

Laser treated surfaces are considered as an alternative treatment to the a-C coating for electron multipacting mitigation. The technology is presently under development for a potential laser treatment of some LHC beam screens [29]. The process offers the advantage to be held under atmospheric pressure but still needs studies to mitigate the dust production and impedance aspects.

In the LHC arcs, a sawtooth structure was produced on the beam screen walls (dipoles and quadrupoles). The structure was designed to intercept the synchrotron radiation at perpendicular incidence to decrease the photoelectron yield and forward scattering of light. Owing to reduced synchrotron radiation in the LSS, such a specific structure was not required for the new HL-LHC beam screens.

12.6.1 Shielded beam screen

The HL-LHC shielded beam screens are to be inserted into the HL-LHC D1, CP and FT of LSS1 and LSS5. These beam screens ensure the vacuum requirements, the shielding of the cold mass from physics debris, and the screening of the 1.9 K cold bore cryogenic system from beam-induced heating.

As a baseline, the shielded beam screen is assumed to fulfil the vacuum requirements with a-C coating operating at a higher temperature than 5-20 K [16]. Recent laboratory studies have demonstrated that a possible operating temperature of the a-C coated shielded beam screen range from 60 to 80 K [30][53].

The selected shielding material is a tungsten heavy alloy, Inermet® 180. It is a sintered tungsten-based composite material with around 95 wt% of tungsten, 3.5 wt% of nickel and 1.5 wt% of copper. The electrical, thermal, magnetic and mechanical properties of the materials from different suppliers have been measured at room and cryogenic temperatures [17]. In the 60–80 K range, Inermet® 180 has an electrical resistivity of 4 10^{-8} Ω.m, a magnetic susceptibility in the order of 10^{-4} and a thermal conductivity of 75 W m^{-1} K^{-1}.

The shielding is made of 40 cm long tungsten alloy blocks, which must be accommodated on the beam screen structure [18]. Figure 12-4 shows a concept based on a mechanical assembly of the tungsten absorbers [19].

As for the standard LHC beam screen, the shell is perforated with oblong holes (slots) to provide sufficient pumping speed of the desorbed gas. These slots are screened by a shield to prevent the cold bore surface from electrons bombardment. The inner side of this electron shield is coated with a-C [28].

The pumping speed of the beam screen slots, computed with Molflow, equals 600 ℓ/s per meter of tube for nitrogen at 20°C. The electron shields reduce this pumping speed to 430 ℓ/s per meter of tube, slightly larger than the LHC arc beam screen-electron shield assembly (365 ℓ/s per meter of tube for nitrogen at 20°C) [31]. The shielded beam screen transparency set to 2% provides a total surface area for the slot of 60 cm^2/m.

The cooling is provided by four 10 mm diameter tubes. Copper strips are installed between the absorbers and the cooling tubes to assure a good heat transfer.

The tungsten blocks are positioned on the beam screen by pins, welded onto the shell. Dedicated slots are used on one side of the block to allow differential thermal contraction.

The beam screen is supported in the cold bore by a titanium spring ceramic ball system [32]. Vibration study has been carried out [33]. Natural frequency of the first mode is expected at around 13 and 20 Hz for the Q1 and Q2, respectively. High damping occurs due to Coulomb friction and magnetic forces.

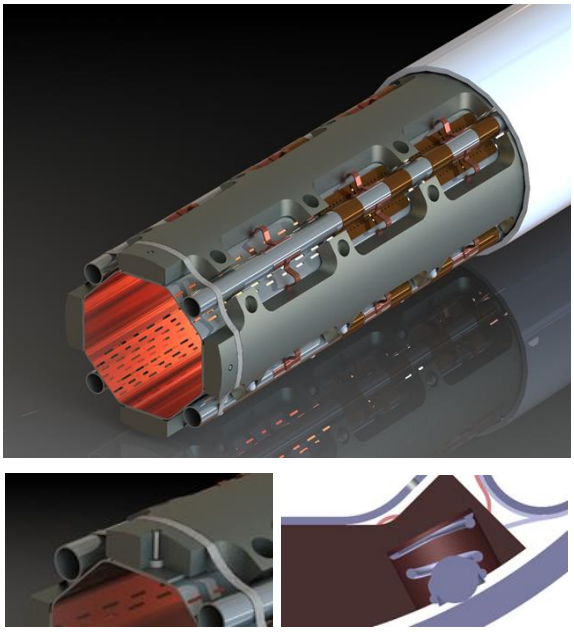

Figure 12-4: Mechanical design of the beam screen with tungsten shielding (for illustration, one electron shield has been removed from the top image to show the slots behind). Top image, cold bore and beam screen assembly, bottom images, details of the tungsten supporting structure (left) and beam screen supporting system (right).

During a magnet quench, the fast decay of the magnetic field leads to the development of Foucault currents that induce Laplace forces, especially in high electrical conductivity material such as copper. A thermomechanical model was developed to study the effect on the structure of a magnet quench [34]. The behaviour of the assembly is driven by the 75 μm thick copper layer and the tungsten alloy absorbers; the typical electrical resistivity is in the order of 2.10^{-10} Ω.m and 4.10^{-8} Ω.m, respectively. The temperature dependence and magneto-resistivity have been considered. Dynamic behaviour and self-inductance effects are implemented in the model as well.

For Q1, the specific resultants of the e.m. forces, per quadrant, are around 40 N/mm and 230 N/mm for the copper layer and tungsten absorbers, respectively.

The beam screen assembly has been designed to be elastic and therefore, during a magnet quench, the tungsten absorbers go in contact with the 4 mm thick cold bore, which can withstand the high magnetic forces. The maximum contact force between the tungsten and the cold bore is around 350 N/mm. The maximum Von Mises stress in the cold bore is around 520 MPa which is below the yield strength (860 MPa). The maximum stress in the beam screen wall is around 580 MPa, whereas the yield stress is around 1150 MPa.

The mechanical assembly is also designed to be compatible with the Coupling Loss Induced Quench (CLIQ) system that is based on a fast transient alternating current unbalanced between the different coils of the magnet. The current evolution being non-monotonic leads to an inversion of the Laplace force direction. For the beam screen and in particular for the tungsten blocks, this induces torques of respectively, 700 N.m and 580 N.m, per beam screen meter, for the absorbers and beam screen tube [35]. The behaviour with fast discharge also in presence of CLIQ has been validated on a Q1 short model test [36].

The heat deposited on the tungsten absorbers is transferred by thermal links to the cooling tubes, in which a helium flow is imposed. The specific thermal load for the whole beam screen is 25 Wm^{-1} and 15 Wm^{-1}, for the Q1 and Q2 beam screens, respectively. A detailed parametric thermal analysis has been also carried out based on [34].

Along the magnet string, the operating temperature windows for the beam screen copper inner layer is 60–80 K. The 20 K temperature increase above the 60 K gas inlet is due for 15 K to the longitudinal temperature gradient along the triplet between Q1 and D1, and for 5 K to the transversal temperature gradient, i.e. between the helium and the copper inner layer. A temperature difference between the helium and the absorbers of up 15.8 K is expected for the Q1 whereas the variation for the copper layer is assessed below 1 K, Figure 12-5.

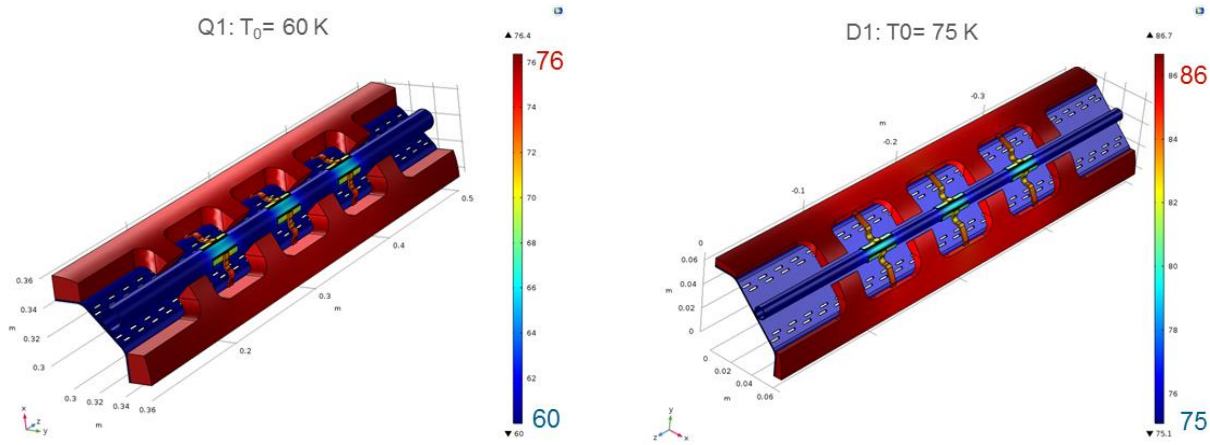

Figure 12-5: Expected temperature field for the Q1 and Q2 beam screens.

The heat transfer is ensured by thermal links in copper, 5 mm^2 cross-section (5 mm width; 1 mm thickness: 2 × 0.2 mm + 6 × 0.1 mm multilayer). Three pairs of links are brazed on the tungsten absorbers. On the other side, an interface plate, 30 mm long, in colaminated copper/P506 stainless steel is welded on

the cooling tube, see Figure 12-6 left side. The thermal behaviour has been assessed on small samples and on a representative 80 cm long beam screen prototype, Figure 12-6, right side.

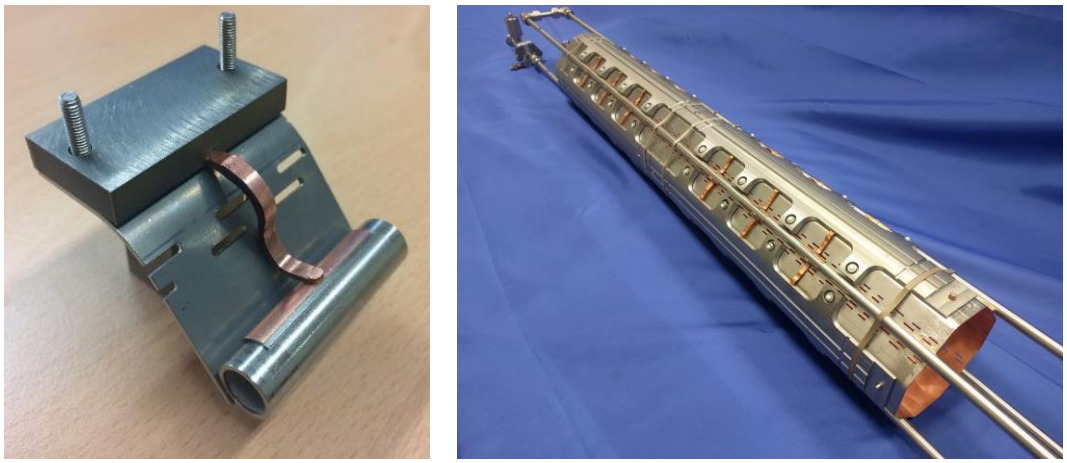

Figure 12-6: Samples and prototype used for the heat transfer assessment.

Different cooling configurations have been considered before selecting the most appropriate one [37]. A good agreement with the simulations has been obtained and a temperature difference between helium and the internal surface of the beam screen tube below 0.5 K has been achieved.

The overall heat load from the beam screens to the 1.9 K cold bore is expected to remain within the cryogenic budget. The heat is transferred by both conduction through the titanium springs and ceramic balls and by radiation. The heat transfer by conduction through the supporting system has been assessed by both simulations and measurements on a dedicated mock-up [54].

A heat load to the cold bore of 5 to 8 m W/spring has been measured for absorber temperatures between 60 to 90 K. Results are in good agreement with simulations [38] and a low dependence with the compression force has been also observed [37]. The laboratory test on the beam screen prototype has confirmed that the heat load to the cold bore remains below the cryogenic budget of 500 m W/m in the HL-LHC operating windows with 50% margin and ultimate conditions. Non-nominal conditions (point-like direct contact between the beam screen and the cold bore, uneven heat loads) have been assessed as well [39].

The main mechanical parameters have been also derived. Table 12-3 summarise the main dimensions and tolerances for the design and construction of the IT, CP and D1 assembly [40].

Table 12-3**:** Cold bores and beams screens main dimensions and tolerances of the IT, CP and D1 assembly of LSS1 and LSS5 [40].

	Cold bore		**Beam screen**						
	Inner Diameter	Thickness	Nominal aperture* H(V) ; ±45º	Vertical tolerance		Horizontal tolerance		Cooling tube Nb×OD×thickness	Shielding maximum Thickness
				Shape	Positioning**	Shape	Positioning**		
Q1	136.7 H8	4 0/+0.5	99.7; 99.7	±1.15	-1.23/+0.15	±1.1	±0.65	4 × 10 × 1	16
Q2a	136.7 H8	4 0/+0.5	119.7; 110.7	±1.15	-1.05/+0.11	±1.1	±0.65	4 × 10 × 1	6
Q2b	136.7 H8	4 0/+0.5	119.7; 110.7	±1.15	-1.05/+0.11	±1.1	±0.65	4 × 10 × 1	6
Q3	136.7 H8	4 0/+0.5	119.7; 110.7	±1.15	-1.05/+0.11	±1.1	±0.65	4 × 10 × 1	6
CP	136.7 H8	4 0/+0.5	119.7; 110.7	±1.15	-1.05/+0.11	±1.1	±0.65	4 × 10 × 1	6
D1	136.7 H8	4 0/+0.5	119.7; 110.7	±1.15	-1.05/+0.11	±1.1	±0.65	4 × 10 × 1	6

* Cu layer thickness, thermal contraction, self-weight deformation not accounted.

** One additional support, 0.25 radial clearance between the support and the cold bore.

The cold bore inner diameter is set to 136.7 mm all along the magnet string. The beam screen nominal aperture is reduced in Q1, positioned at 40 m from the interaction point, to allow the insertion of thicker tungsten shielding for better magnets protection.

Finally, The magnetic frequency response of the shielded beam screen was studied in detail for the specification of the power converter performance [41].

12.6.2 Non-shielded beam screen

The HL-LHC non-shielded beam screens are to be inserted into the HL-LHC D2, Q4 and non-crabbed lines of LSS1 and LSS5. If needed, new beam screens will be inserted in Q5 and Q6 of LSS1 and LSS5 and D1, DFBX, and IT of LSS2 and LSS8. Such beam screens (equipped with hydrogen cryosorbers when used for the 4.5 K cold masses of Q4, Q5 and Q6 [42]) ensure the vacuum requirements together with screening of the cold bores from beam-induced heating.

As a baseline, the a-C beam screen is assumed to fulfil its vacuum requirements with a-C coating operating at 5–20 K [16].

Table 12-4 gives the main dimension of the cold bore and beam screens of the LSS1 and LSS5 for the present designs of D2 and the non-crabbed line and for Q4, Q5 and Q6 based on the LHC design [43]. All beam screens, except Q6, are a-C coated. The beam screens of Q5 and Q6, equipped with hydrogen cryosorbers, are recovered from the LHC matching section.

Table 12-4**:** Cold bores and beams screens main dimensions and tolerances of the D2, non-crabbed line, Q4, Q5 and Q6 assemblies of the LSS1 and LSS5 [43].

Machine	**Cold bore**		**Beam screen**			
	ID/OD	**ID tolerance**	**a-C coated**	**Shape**	**H(V); ±45º ID/OD**	**Radial ID; Between flats ID**
D2	94.5/100	1.10	Yes	Non regular octagonal	87.4; 77.6	-
Non-crabbed line	84/88	0.20	Yes	circular	69.9/72.1	-
Q4	62.98/66.5	0.38	Yes	racetrack	-	57.8; 48.0
Q5	50/53	0.35	Yes	racetrack	-	45.1; 35.3
Q6	50/53	0.35	No	racetrack	-	45.1; 35.3

12.6.3 Vacuum beam line interconnection

The HL-LHC shielded beam screens are to be inserted into the HL-LHC D1, CP and IT region of LSS1 and LSS5. Beam vacuum interconnections ensure the continuity of the beam vacuum envelope, a smooth transition between adjacent beam screens, and the electrical continuity of the image current.

Figure 12-7 shows the present design of the vacuum beam line interconnection (length = 1000 mm) which integrate a non-deformable RF bridge and tungsten shielding for better cold mass protection against the debris produced at the IP [47].

The beam screens are fixed on one side to the cold mass; on the other side, compensation bellows between the beam screen extremity and the cold mass has to be integrated to cope with the differential thermal displacements between the beam screens and the cold mass.

The four 10 mm diameter cooling tubes are routed along the interconnect, connecting the upstream to the downstream beam screen. Through-wall welds on the helium circuit are forbidden in the beam vacuum. Automatic welds have to be used in the insulation vacuum.

A new type of non-sliding RF fingers (deformable RF bridge) are implemented and are being developed [44].

The vacuum beamline interconnections in the triplets integrate BPMs as well.

A tungsten shielding is also integrated into the interconnection around the beam position monitor body and at the beam screen extremity on the non-IP side to further increase the protection of the cold mass against the collision debris [45].

Finally, a-C coating of the vacuum beam interconnection is required to reduce the beam-induced heat load on the cryogenic system [46]. For this purpose, the coating of the interconnection line, including for the BPM body and the deformable RF bridge, will be done in the laboratory during the construction phase.

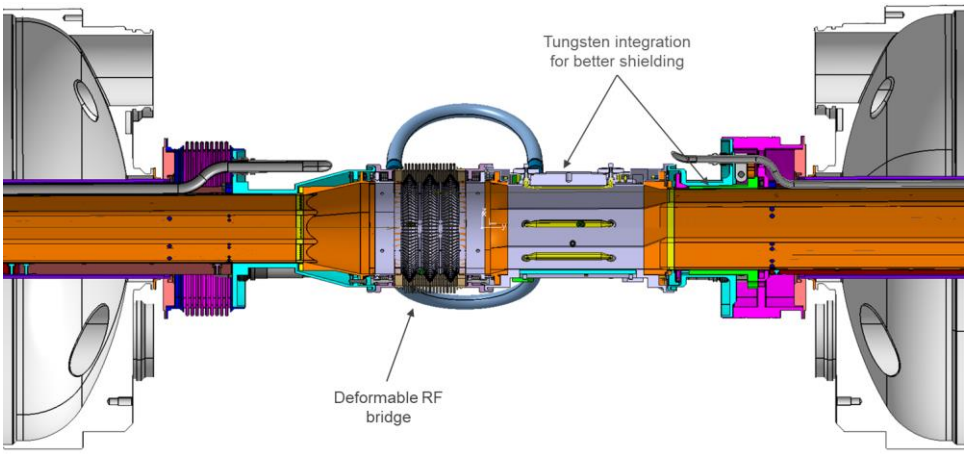

Figure 12-7: Vacuum beam line interconnection [44].

12.6.4 Cold-to-warm transitions

The HL-LHC cold-to-warm transitions design are based on the LHC machine. They are placed at each cryostat extremity. They must be made of a rigid tube to avoid the introduction of a RF bridge in the cryostat. For this reason, a bellow is welded at the external envelope of the cryostat to compensate from the cold mass length contraction during cool-down. The maximum acceptable length without beam screen shall be less than 1 m to prevent from pressure runaway. Therefore, longer cold-to-warm transitions require specific designs to satisfy this condition. The cold-to-warm transition of beam screen operating in the 5–20 K range, shall be thermally anchored to the cryostat thermal screen. Other cold-to-warm transitions designed for beam screens operating at higher temperature (60–80 K) do not require thermal anchoring to the cryostat thermal screen.

At present, the Q1 cold-to-warm transition integrates a beam position monitor. The D1 cold-to-warm transition is placed after at an extension of the helium vessel designed to provide vacuum pumping. Cold-to-warm transitions at other locations are under study.

12.7 References

[1] L. Rossi, Status of HiLumi: from design study to construction project, 5th Joint HiLumi LHC-LARP Annual Meeting 2015, INDICO: 400665.

[2] O. Gröbner, Overview of the LHC vacuum system. *Vacuum* **60**, 2001, DOI: 10.1016/S0042-207X(00)00240-2.

[3] LHC Design Report, 2004, DOI: 10.5170/CERN-2004-003-V-1.

[4] A. Rossi, Residual Gas Density Estimations in the LHC Insertion Regions IR1 and IR5 and the Experimental Regions of ATLAS and CMS for Different Beam Operations, 2004, LHC Project Report 783.

[5] A. Rossi, Residual gas density estimations of the LHC experimental interaction regions. CERN LHC Project Report 674 (2003), EDMS: 410413.

[6] Model of LSS layout LHCLJV_L0011, EDMS: 356208.

[7] ATLAS vacuum layout Q1/Q1. LHCVC1__0007, EDMS: 1317281.

[8] CMS LS2 vacuum layout Q1/Q1. LHCVC5__0009, EDMS: 1992313.

[9] J. Sestak, LHC experimental beam vacuum consolidation and upgrade ATLAS experiment, EDMS: 2234763.

[10] J. Sestak, LHC experimental beam vacuum consolidation and upgrade CMS experiment, EDMS: 2234765.

[11] ALICE vacuum layout Q1/Q1. LHCVC2__0008, EDMS: 2046454.

[12] J. Sestak, LHC experimental beam vacuum consolidation and upgrade LHCb experiment, EDMS: 2234767.

[13] LHCb vacuum layout Q1/Q1. LHCVC8B_0151, EDMS: 932121.

[14] J. Sestak, LHC experimental beam vacuum consolidation and upgrade ALICE experiment, EDMS: 2234762.

[15] C. Adoriso, HL-LHC residual dose rate estimations in the LSS1 and LSS5 (from TAXS up to Q7), 7th HL-LHC Annual Meeting, Madrid, Spain, EDMS: 1868872.

[16] HL-LHC Decision Management: Temperature beam screens Q1 to Q6. EDMS: 1601082.

[17] C. Garion *et al.*, Material characterisation and preliminary mechanical design for the HL-LHC shielded beam screens operating at cryogenic temperatures, Advances in Cryogenic Engineering - Materials: International Cryogenic Materials Conference, Tucson, AZ, USA, 28 Jun - 2 Jul 2015. DOI: 10.1088/1757-899X/102/1/012013.

[18] C. Garion *et al.*, Preliminary design of the high-luminosity LHC beam screen with shielding, 6th International Particle Accelerator Conference, 2015, DOI: 10.18429/JACoW-IPAC2015-MOBD1.

[19] R. Kersevan *et al.*, Preliminary design of the HiLumi-LHC triplet area beam screen. 5th International Particle Accelerator Conference, Dresden, Germany, 2014, DOI: 10.18429/JACoW-IPAC2014-WEPME048.

[20] V. Baglin, G. Riddone, The spare needs for HL-LHC: what is needed that is not covered yet by the LHC spare policy / HL_LHC operation, EDMS: 2045659.

[21] R. Tavares Rego, HL-LHC Vacuum Layout LSS5, EDMS: 2045739.

[22] P. Santos Diaz, J. Hansen, IP1&5 recombination chamber conceptual design, EDMS: 1824656.

[23] P. Costa Pinto et al. ECR: Amorphous carbon coating in standalone magnets of the LHC in IR2 and IR8 during LS2, EDMS: 1983116.

[24] S. Antipov, Impact of a-C coating on impedance, 124th HiLumi WP2 Meeting, INDICO:741104.

[25] V. Baglin *et al.*, Vacuum System in: High-Luminosity Large Hadron collider (HL-LHC) Preliminary Design Report pp. 195-205, DOI: 10.5170/CERN-2015-005.195.

[26] R. Salemme et al., Vacuum performance of amorphous carbon coating at cryogenic temperature with presence of proton beams. Proc. of IPAC 2016, DOI: 10.18429/JACoW-IPAC2016-THPMY007.

[27] A. Krasnov *et al*, Results on a-C tubes subjected to synchrotron radiation, 8th HL-LHC Annual Meeting, CERN, Geneva, Switzerland, INDICO:742082.

[28] V. Baglin, P. Chiggiato. Preparation of the ECR regarding the modification of the HL-LHC base line for a-C coating. 46th HL-LHC Technical coordination Committee, INDICO:705929.

[29] M. Sitko *et al*. Towards the implementation of laser engineered surface structures for electron cloud mitigation, Proc. of IPAC 2018, Vancouver, Canada, DOI: 10.18429/JACoW-IPAC2018-TUZGBE3.

[30] V. Baglin, Towards final validation of new temperature of beam screen for triplets, 8th HL-LHC Annual Meeting, CERN, Geneva, Switzerland, INDICO:742082.

[31] R. Kersevan. Private communication, September 2018.

[32] C. Garion, Design and behaviour of 3D printed elastic components for HL-LHC shielded beam screen, EDMS: 2001118.

[33] C. Garion, Vibrations of the HL-LHC shielded beam screens, EDMS: 2031211.

[34] M. Morrone, Thermomechanical study of complex structures in the aperture of superconducting magnets: application to the design of the High-Luminosity LHC shielded beam screen, CERN-THESIS-2018-052.

[35] C. Garion, Design and tests of the shielded beam screen, 7th HL-LHC Annual Meeting, Madrid, Spain, INDICO: 647714.

[36] M. Morrone, Quench test of the HL-LHC beam screen in the MQXFS4b magnet, TE Technical Meeting, CERN, Geneva, Switzerland, INDICO: 776870.

[37] P. Borges de Sousa et al, Parametric study on the thermal performance of beam screen samples of the High-Luminosity LHC Upgrade, IOP Conf. Ser. Mater. Sci. Eng. 278, 2017, DOI: 10.1088/1757-899X/278/1/012053.

[38] C. Garion, Design and tests of the shielded beam screen, 7th HL-LHC Annual Meeting, Madrid, Spain, INDICO: 647714.

[39] P. Borges de Sousa, Thermal qualification of the HL-LHC beam screens for the inner triplets, TE Technical Meeting, CERN, Geneva, Switzerland, INDICO: 762917.

[40] C. Garion, Mechanical design of the triplet cold bore and beam screen, 6th HL-LHC Annual Meeting, Paris, France, INDICO: 549976.

[41] M. Morrone *et al*, Magnetic frequency response of High-Luminosity Large Hadron Collider beam screens, Phys. Rev. Accel. Beams 22, 2019, DOI: 10.1103/PhysRevAccelBeams.22.013501.

[42] Full Remote Alignment Study (FRAS) And Matching Section Optimization Targets, and advancement report, P. Fessia et al. 54th HL-LHC Technical Coordination Committee, CERN, INDICO: 747490

[43] N. Kos *et al*, Beam screen for the LHC long straight sections, EDMS: 334961.

[44] C. Garion, Design of the compensation system for the HL-LHC cold beam vacuum interconnections, EDMS: 2012795.

[45] F. Cerutti *et al*, Recap of energy deposition and radiation damage, 7th HL-LHC Annual Meeting, Madrid, Spain. INDICO: 647714.

[46] G. Iadarola *et al*, Beam induced heat loads on Hl-LHC beam screens, 7th HL-LHC Annual Meeting, Madrid, Spain, INDICO: 647714.

[47] C. Garion, Status of beam screen, cold bore, interconnect and CWT design & production, 8th HL-LHC Annual Meeting, CERN, Geneva, Switzerland, INDICO: 742082.

[48] V. Baglin and G. Riddone, HL-LHC WP12 Vacuum & Beam Screen technical update, 99th HL-LHC Technical Coordination Committee, EDMS: 2363271.

[49] R. Tavares Rego, General methodology for vacuum equipment mechanical aperture computation, EDMS: 1999375.

[50] P. Fessia, H. Mainaud Durand, Functional specification full remote alignment system, EDMS: 2166298.

[51] V. Baglin, J. Hansen, G. Riddone, Vacuum: full remote alignment system. Review of HL-LHC alignment and internal metrology, CERN, 25th August 2019, EDMS: 2219953.

[52] V. Baglin. Shielded beam screens operating temperature for the triplets, corrector package and D1, EDMS: 2112891.

[53] V. Baglin, A. Carvalho, G. Riddone, Vacuum for HL-LHC CC. International review of the crab cavity system design and production plan for the HL-LHC, CERN, 19-21 June 2019, INDICO: 787363

[54] P. Borges de Sousa *et al*, Study on heat transfer between the High-Luminosity LHC beam screens and the He II cooled beam tube. IOP Conf. Ser.: Mater. Sci. Eng. 502, 2019, DOI: 10.1088/1757-899X/502/1/012088.